Autonomous Compressive Sensing Augmented Spectrum Sensing

Xingjian Zhang, *Student Member, IEEE,* Yuan Ma, *Member, IEEE,* Yue Gao, *Senior Member, IEEE,*
and Wei Zhang, *Fellow, IEEE*

Abstract—This paper proposes a new spectrum sensing technique, referred to as autonomous compressive sensing (CS) augmented spectrum sensing, which can be developed to provide more efficient spectrum opportunities identification than geo-location database methods. Firstly, we propose an autonomous CS-based sensing algorithm that enables the local secondary users (SUs) to automatically choose the minimum sensing time without knowledge of spectral sparsity or channel characteristics. The compressive samples are collected block-by-block in time while the spectral is gradually reconstructed until the proposed stopping criterion is reached. Moreover, a CS-based blind cooperating user selection algorithm is proposed to select the cooperating SUs via indirectly measuring the degeneration of signal-to-noise ratio (SNR) experienced by different SUs. Numerical and real-world test results demonstrate that the proposed algorithms achieve high detection performance with reduced sensing time and number of cooperating SUs in comparison with the conventional compressive spectrum sensing algorithms.

Index Terms—Compressive sensing, cognitive radio, wideband spectrum sensing, spectrum access framework.

I. INTRODUCTION

Regulatory bodies worldwide are facing that the rapid growth of wireless communication industry is overwhelming current static spectrum supply, and thus encourages an urgent need for improved spectrum assignment strategy to mitigate the gap between the available spectrum and the demand [1], [2]. A key finding of the U.S. 2012 President's Council of Advisers on Science and Technology (PCAST) report [3] is that advanced spectrum sharing technologies have the potential to "transform spectrum scarcity into abundance" based on the following two factors: first, it is well recognised that many licensed frequency bands are under-utilized in practice either over time or geography locations [4]; second, there have been some rapid advances towards the development of dynamic spectrum access such as cognitive radio technology [5]–[7]. To that end, the academia, industry, and regulatory bodies are closely collaborating to pursue policy and technology

Xingjian Zhang, Yuan Ma and Yue Gao are with the School of Electronic Engineering and Computer Science, Queen Mary University of London, London E1 4NS, U.K. (emails:{xingjian.zhang, y.ma, yue.gao}@qmul.ac.uk).
Wei Zhang is with the School of Electrical Engineering and Telecommunications, University of New South Wales, Sydney, NSW 2052, Australia (e-mail: wzhang@ee.unsw.edu.au).

innovations based on the paradigm of the *shared spectrum*. Recently, the 3550-3700 MHz (referred to as 3.5 GHz band) Citizens Broadband Radio Service (CBRS), is considered for the spectrum sharing by Federal Communications Commission (FCC) in the US. Meanwhile, UK Office of Communications (Ofcom) has published the call for input [8] which considers the 3.8 GHz to 4.2 GHz as the first band where they apply the spectrum sharing framework. In order to share the spectrum efficiently and limit the interference among users, three-tiered spectrum access framework was introduced in the above-mentioned shared spectrums [9], [10], where the incumbent users as the primary users (PUs) operate at the top tier, while the CBRS users as the secondary users (SUs) operate at the second or third tiers holding priority access license (PAL) or generalized authorized access (GAA), respectively. Each tier accepts interference from tiers above and is protected from tiers below.

One of the vital important parts of the three-tiered spectrum access framework is how to identify available spectrum bands while protecting the operation of existing users. The current shared spectrum access systems either utilize geo-location database to determine which portion of the spectrum is unoccupied or make use of environmental sensing capability (ESC) system to sense the presence of the incumbent users [4]. Based on the experience of the TV white space (TVWS) database operation [11], the existing geo-location database technology is capable of facilitating the three-tiered access to the shared spectrum [12]. However, some of the PUs' spectrum usage information provided by database might be missed or out of date. Besides, the database only protects the communication of the PUs. Therefore, both of the PUs and the SUs may suffer from severe interference and some spectrum opportunities are not efficiently utilized [13]. ESC is a group of RF sensors and a decision system deployed in the coastal areas, which is designed to detect the presence of the shipborne incumbent users [14]. However, ESC sensors are normally deployed close to the ocean, which may be far from many metropolitan areas. Moreover, ESC sensors should be deployed with a desired level of redundancy to maintain fault tolerance to sensor outage.

In contrast, the sufficient amount of the CBRS access points as the SUs are widely deployed to provide secondary spectrum access in both urban and rural areas, which could be the nearest infrastructures to most user devices. Therefore, the Citizens Broadband Service Device (CBSD) sensing network, which consists of CBRS access points and CBRS users with sensing capability, is an ideal solution for identifying the

spectrum opportunities [4]. Remarkably, there are two key challenges to realize the CBSD sensing network in three-tiered spectrum sharing framework.

Firstly, to make the best of the shared spectrum, a wide portion of the spectrum must be sensed (up to 400MHz in UK spectrum sharing framework [10]). Since the sampling rate of A/D converters in the SUs should be higher than twice of spectrum bandwidth due to the Nyquist-Shannon's sampling theorem, the A/D converters with very high sampling rate must be employed and large amounts of spectrum data have to be processed afterwards, which is unrealistic to be installed in the commercial SUs with restricted energy resources, e.g., mobile sensors and IoT devices. To alleviate the bottleneck of high rate A/D converters and the massive data processing burden after sampling, compressive sensing (CS) [15], [16] was applied to acquire wideband signals using the lower sampling rates than Nyquist rates by exploiting the sparse nature of the wideband spectrum as shown in Fig. 1. Due to the shorter propagation distance as the result of higher central frequencies (3.5GHz or above) used in three-tiered spectrum access framework, most spectrum occupancy status varies with users accessing or releasing the spectrum randomly. Therefore, the sparsity of the wideband signals is also varying and unknown [17]. Conventional CS theory requires prior knowledge of signal sparsity to calculate the sufficient number of compressive samples for signal reconstruction. Since the sparsity level is often unknown in practice, most of CS approaches assume a large sparsity level and choose the excess number of compressive samples to guarantee the quality of reconstruction. It turns out that these approaches require more sensing time or higher sampling rates to collect compressive samples, which causes larger sensing latency and therefore loses the advantage of using CS technologies.

Secondly, to overcome the signal-to-noise ratio (SNR) degeneration caused by multi-path fading, shadowing, and random noise over wireless channels, cooperative spectrum sensing (CSS) has been shown to increase the reliability of sensing by exploiting the spatial diversity across the multiple SUs [18], [19]. However, a large number of the SUs participating in CSS network leads to extensive energy consumption and transmission overhead due to sensing reporting and sensing decision at the fusion center. Therefore, only the SUs with high detection capabilities should be selected. It is shown in [20] that the best detection performance is usually achieved by cooperating only with the SUs that have the highest SNR values. In general, the SNRs experienced by the different SUs are unknown in advance, so that it is hard to identify SUs which have the best detection capability.

Motivated by the above challenges, the contribution of this paper is two-fold.

1) Firstly, in order to reduce both the sensing time and data processing burden, and provide the exact signal reconstruction without any extra channel assumption including prior knowledge of sparsity, we propose an autonomous CS-based sensing algorithm that enables the local SUs to choose the number of compressive samples automatically. More specifically, instead of assuming the upper limit of sparsity level, which would not take
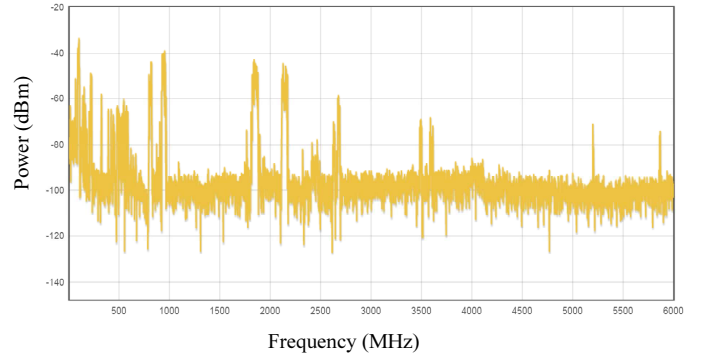

Fig. 1. The real-time spectrum occupancy recorded at QMUL (51.523021°N 0.041592°W). The figure shows that the spectrum is sparsely occupied on $\mathcal{F} = [0, 6000]$ MHz.

the full advantage of CS due to redundant samples collection, the proposed algorithm can autonomously terminate the samples acquisition when the proposed Euclidean distance D_p is smaller than a given threshold. The proposed algorithm could therefore achieve the minimum sensing time under the given sampling rate.

2) Secondly, we propose a CS-based blind cooperating user selection algorithm over wide spectrum without any prior knowledge of the primary signals, sensor locations. More specifically, by observing the reconstruction error of CS is degraded with the SNR experienced by SUs, i.e., lower SNR leading to larger reconstruction error under given sampling rate and sensing time, the proposed algorithm employ the same mechanism as the proposed autonomous CS-based sensing algorithm to indirectly compare the degenerating of SNRs according to the approximated reconstruction errors.

Additionally, performance analysis of the proposed autonomous CS augmented spectrum sharing scheme is presented to show its efficiency on dynamic spectrum sharing. Furthermore, the proposed algorithms are tested by the simulated signals as well as the real-world signals.

The rest of this paper is organized as follows: Section II discusses the related work on spectrum sensing. In Section III, the preliminary system and signal model is described. Section IV introduces the proposed autonomous CS-based sensing algorithm. Section V develops the proposed blind cooperating user selection algorithm for selecting SUs with high SNR. Section VI analyzes and validates the proposed algorithms over simulated and real-world TVWS signals. Conclusions are drawn in Section VII.

II. RELATED WORK

Recently, there are some works employing CS into spectrum sensing. In [21] and [22], novel frequency-domain cyclic prefix (CP) autocorrelation based compressive spectrum sensing algorithms were proposed to detect PUs in the presence of noise uncertainty and frequency selectivity. By making use of sparsity in the spectral domain, CS was utilized to construct the autocorrelation of the received signal from its subband sample sequences. In [12] and [23], hybrid frameworks are

proposed to incorporate the advantages of both geolocation database and CS-based spectrum sensing. However, the aforementioned works require the prior knowledge such as instant sparsity level of the wideband spectrum for signal reconstruction. Therefore, to eliminate the prior knowledge of instant spectral sparsity level in CS-based spectrum sensing. Authors in [24] proposed a sparsity order estimation method to obtain the minimum sampling rate. To further improve the sparsity order estimation performance, a dynamic sparsity upper bound adjustment scheme was proposed in [25] for obtaining a proper sparsity upper bound. Compared with these algorithm, the proposed autonomous CS-based sensing algorithm can automatically choose the number of compressive samples without any sparsity estimation efforts.

To solving the cooperating SUs selection problem in spectrum sharing framework, with the knowledge of the SUs' locations, the authors in [26] addressed the user selection problem by selecting a set of SUs which experience uncorrelated shadow fading. The knowledge of the distance between SUs and base station is required by those algorithms which also need the central coordination, i.e., the sensing results should be sent to the fusion center for selection. In [27], without the prior knowledge of the SUs' locations, three methods for selecting the SUs based on hard local decisions were proposed, which outperform the purely random selection method of SUs. Moreover, a correlation-aware user selection scheme was proposed in [28], which was developed by adaptively selecting the SUs based on the evaluation of the correlation experienced by the SUs. However, the aforementioned algorithms are under the circumstance of narrowband sensing rather than wideband one and therefore are not suitable for wideband CSS. In [29], a hybrid double threshold based CSS scheme was proposed, which could improve the detection performance at SUs by exploiting both local decisions and global decisions feedback from the fusion center. Based on order statistic information of the reporting links between SUs and fusion center, a multi-selective sensing scheme was proposed in [18]. The links with high SNRs are selected and the number of selected links is decided centrally. Although the two schemes could be applied in wideband CSS, the selection process would be inefficient since the schemes introduce large latency due to the sequential manner of sensing. Our proposed blind user selection algorithm in this paper could capture the whole wide spectrum at the same time based on CS but utilizes a few compressive samples to select the SUs with high detection capabilities.

III. SYSTEM AND SIGNAL MODELS

In this section, the preliminary system and signal models of the proposed autonomous CS augmented spectrum sharing scheme are presented.

A. System Model

In the conventional three-tiered spectrum access framework, the responsibility of the spectrum access system (SAS) is to manage all the incumbent and secondary operations based on the information obtained from the incumbent database and
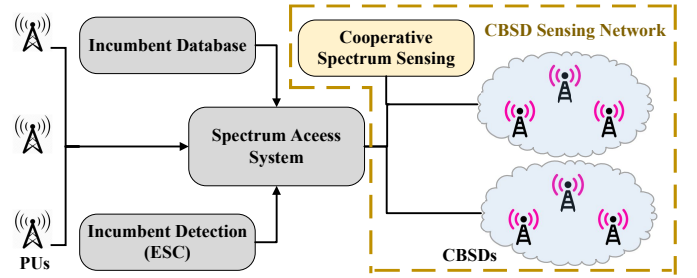

Fig. 2. The proposed sensing-augmented spectrum sharing architecture

the incumbent detection, i.e., ESC. The incumbent database provides all the necessary spectrum usage and operational information of the incumbent users. ESC detects the presence of shipborne incumbent users with a group of RF sensors and the interference from the unregistered users. As shown in Fig. 2, the proposed scheme adopt the CBSD sensing network that consists of the CBRS access points and the CBRS users with sensing capability to identify spectrum opportunities and the unregistered users operating on the target spectrum. Moreover, due to the centralized nature of SAS and the availability of the multiple SUs, the proposed scheme can utilize the CSS scheme over the SUs within the same secondary access network to deal with the issues such as multi-path and shadowing, which also can increase the spatial diversity and reduce the probability of deep fading across all the SUs.

B. Signal Model

Sensing in the three-tiered spectrum access framework aims to find the spectrum holes which could be used for secondary access and identify the unwanted interference event over the whole shared spectrum. Let $x(t)$ be a real-valued continuous-time signal received at the RF front end of the local SU, such that

$$x(t) = \sum_{i=1}^{N_{\text{sig}}} s_i(t) + n(t), \tag{1}$$

where N_{sig} is the number of ongoing transmission signals which span over the total band of W Hz, $s_i(t)$ is the i-th signal and $n(t)$ refers to additive white Gaussian noise with zero mean and variance σ_n^2. In the conventional Nyquist sampling system, we could obtain a discrete time sequence $x[k] = x(\frac{k}{f_N})$, $k = 0, 1, \ldots, N-1$ by using the Nyquist sampling rate f_N over the total sensing time T_N. N is the number of Nyquist samples as $N = f_N \cdot T$, $N \in \mathbb{Z}$.

Based on the Nyquist sampling theory, the sampling rate f_N is required to be higher than $2W$ samples per second and therefore a lot of samples would be generated to process, which slow down the processing speed and cause large power consumption. Therefore, such Nyquist sampling rate schemes over wideband spectrum are likely unrealistic to be implemented in the commercial SUs. This predicament urges us to apply CS technologies to reduce the number of samples while remaining the total bandwidth W unchanged.

In a CS-based spectrum sensing approach, the main task is to reconstruct $x[k]$ or its discrete Fourier transform (DFT)

$\boldsymbol{x} = \{(x_1, x_2, \ldots, x_N)^T)| \ \boldsymbol{x} \in \mathbb{R}^N\}$ from compressive samples. Specifically, since the wideband spectrum is practically under-utilized, $x(t)$ typically bears a sparse property in the frequency domain such that its DFT $\boldsymbol{x} \in \mathbb{R}^N$ is a k-sparse vector, i.e., $|\{x_i \ : \ x_i \neq 0\}| \leq s$. Therefore, the wideband spectrum signal acquisition could be accomplished with a sub-Nyquist sampling rate $f_s < 2W$, resulting in fewer samples, and $x[k]$ or $\boldsymbol{x}$ could be reconstructed from the compressive samples [30], which is expressed by the following analytical model:

$$\boldsymbol{y} = \boldsymbol{\Phi}\boldsymbol{x} + \boldsymbol{\xi} \quad \text{subject to } ||\boldsymbol{x}||_0 \leq s, \tag{2}$$

where $\boldsymbol{\Phi} \in \mathbb{R}^{M \times N}$ is the measurement matrix to collect the compressive samples $\boldsymbol{y} \in \mathbb{R}^M$ from the original signal $\boldsymbol{x}$, which could be implemented using sub-Nyquist samplers, e.g., random demodulator [31] and modulated wideband converter [32], in which controllable measurement matrices have been proposed to realize CS. $M \in \mathbb{Z}$ (with $s < M < N$) refers to the dimension of $\boldsymbol{y}$, and $|| \cdot ||_0$ represents the number of nonzero elements in the vector, which is also treated as the measure of sparsity. The compressive ratio in this compressive signal acquisition is given by $\rho = M/N < 1$ and total sensing time $T_s = M/f_s$. $\boldsymbol{\xi} \in \mathbb{R}^M$ is the noise perturbation, whose magnitude is constrained by an upper bound δ, i.e., $||\boldsymbol{\xi}||_2 < \delta$.

IV. THE PROPOSED AUTONOMOUS CS-BASED SENSING ALGORITHM

In this section, we present an autonomous CS-based sensing algorithm applied in local SUs of the CBSD sensing network.

A. Algorithm description

In CS theory, the number of compressive samples M is chosen regarding the sparsity level s of the signal in order to guarantee the quality of reconstruction, e.g., $M \geq Cs\log(N/s)$ for a Gaussian measurement matrix, where C denotes a constant [15]. The sparsity level s of the spectrum is assumed to be known in most of the CS-based spectrum sensing approach. These approaches intend to assume a maximum sparsity level $s_{\max}$ to ensure a high successful recovery rate since the sparsity level is often unknown and fluctuates in practice. Therefore, the required number of compressive samples is larger than the necessary amount, which causes unnecessary sensing latency or higher sampling rate for collecting extra samples.

In contrast, our autonomous CS-based sensing algorithm is adaptive to actual sparsity level, where the sensing time T_s is divided into several time intervals and the wideband signal is acquired block-by-block in time until the stopping criterion regarding reconstruction accuracy is reached. Therefore, the waste of samples can be averted and the sensing latency or sampling rate could be further reduced. Additionally, the remaining sensing time can be utilized for data transmission.

Specifically, the proposed algorithm divides the total sensing time T_s into P time intervals where p ($p \in [1, P]$) refers to the index of each time intervals. Let $\boldsymbol{y_p}$ represents a vector contains all the samples which are collected until the end of the p-th time interval, and M_p denotes the number of elements in vector $\boldsymbol{y_p}$, where $0 < M_1 < \cdots < M_p$. $\boldsymbol{\Delta y_p}$ and ΔM

represent a vector contain the samples collected during the p-th time interval and the number of samples collected in each time interval, respectively, i.e., $\Delta M = M_p - M_{p-1}$.

The collected samples vector $\boldsymbol{y_p}$ could be utilized for signal reconstruction by solving the l_1-norm minimization problem:

$$\underset{\boldsymbol{x_p} \in \mathbb{R}^N}{\arg\min} ||\boldsymbol{x_p}||_1 \quad \text{subject to } ||\boldsymbol{\Phi_p}\boldsymbol{x_p} - \boldsymbol{y_p}||_2^2 \leq \delta, \tag{3}$$

where $\boldsymbol{\Phi_p}$ denotes a $M_p \times N$ matrix and $\boldsymbol{x_p}$ is the reconstructed signal from $\boldsymbol{y_p}$. The original wideband spectrum signals tend to be compressible rather than sparse in the real-world environment, which can be well approximated by sparse signals, but the reconstruction errors can only be diminished but not vanished [33]. Therefore, we utilize a proper constant parameter $\lambda \in \mathbb{R}^+$ to balance the objective of minimizing the reconstruction error and the solution sparsity according to the Lagrange multiplier theorem, such that the problem (3) could be equivalently solved by the following unconstrained optimization problem:

$$\underset{\boldsymbol{x_p} \in \mathbb{R}^N}{\arg\min} ||\boldsymbol{\Phi_p}\boldsymbol{x_p} - \boldsymbol{y_p}||_2^2 + \lambda||\boldsymbol{x_p}||_1. \tag{4}$$

In addition, the choice of λ depends on the noise level of the original signal, e.g., the value of λ should be increased when the noise floor is higher [34].

As the fewer measurements are usually required for the l_ν-norm minimization approach compared with the l_1-norm minimization approach [35], we consider the approximation of the l_0-norm by the l_ν-norm instead of the l_1-norm in (4):

$$\underset{\boldsymbol{x_p} \in \mathbb{R}^N}{\arg\min} ||\boldsymbol{\Phi_p}\boldsymbol{x_p} - \boldsymbol{y_p}||_2^2 + \lambda||\boldsymbol{x_p}||_\nu^\nu. \tag{5}$$

In contrast to the l_1-norm, the l_ν-norm with $0 < \nu < 1$ is nonconvex. As convex optimization techniques are no longer applicable, the global minimizer is not guaranteed and general NP-hard due to the nonconvexity of the l_ν-norm minimization. To that end, iterative reweighted least square (IRLS) algorithm was proposed to solve this problem by solving a sequence of the approximation subproblems [36]. The solution sequence generated by the IRLS algorithm converges to the local minimum as the sparsest solution which is also the actual global l_ν-norm minimizer under certain assumptions such as the null space property (NSP) on $\boldsymbol{\Phi_p}$ [35]. However, the computational burden of l_ν-norm minimization is higher than that of l_1-norm minimization. To reduce the iterations and speed up the convergence of reconstruction, we adopt the adaptively regularized iterative reweighted least square (AR-IRLS) reconstruction algorithm [37] which moves the estimated solutions along an exponential-linear path by regularizing the weights in each iteration with a series of non-increasing penalty terms. Specifically, the iterative estimates $\{\boldsymbol{x_p}^{(l)}\}_{l=1}^\infty$ of $\boldsymbol{x_p}$ is given by

$$\boldsymbol{x_p^{(l)}} := \underset{\boldsymbol{x_p} \in \mathbb{R}^N}{\arg\min} ||\boldsymbol{\Phi_p}\boldsymbol{x_p} - \boldsymbol{y_p}||_2^2 + \lambda||\boldsymbol{x_p}||_2^{2(\boldsymbol{w_p^{(l)}})},$$
$$\boldsymbol{w_p^{(l)}} := (w_{p(1)}^{(l)}, \ldots, w_{p(N)}^{(l)}), \tag{6}$$

where $||\boldsymbol{x}||_2^{2(\boldsymbol{w})}$ denotes $\sum_{i=1}^N w_i x_i^2$ and $w_{p(j)}^{(l)}$ is defined as

$$w_{p(j)}^{(l)} = \left(\left(x_{p(j)}^{(l-1)}\right)^2 + \epsilon\right)^{\frac{\nu}{2}-1} \quad 0 < \nu < 1. \tag{7}$$

Algorithm 1 Autonomous CS-based sensing algorithm

Require: Equally divide the total spectrum sensing time T_s into P time intervals and set the start time interval index $p = 1$. Sampling rate f_s, number of samples ΔM collected in each time interval and the reconstruction error threshold κ.

Ensure: The reconstructed signal $\boldsymbol{x}^*$

1: **for** $p = 1, \ldots, P$ **do**

2:     Sampling the wideband signal using f_s till the time interval $p + 1$ so as to obtain the compressive samples vector $\boldsymbol{y_p}$ and the samples $\Delta \boldsymbol{y_{p+1}}$ collected in time interval $p + 1$.

3:     Reconstruct the spectral from $\boldsymbol{y_p}$ by utilizing AR-IRLS algorithm to solve the l_ν-norm minimization problem

$$\arg \min_{\boldsymbol{x_p} \in \mathbb{R}^N} ||\boldsymbol{\Phi_p} \boldsymbol{x_p} - \boldsymbol{y_p}||_2^2 + \lambda ||\boldsymbol{x_p}||_\nu^\nu,$$

which leads to a spectral reconstruction $\boldsymbol{x_p}$.

4:     Calculate the proposed Euclidean distance

$$D_p = ||\boldsymbol{\Phi_{\Delta M}} \boldsymbol{x_p} - \Delta \boldsymbol{y_{p+1}}||_2^2$$

5:     **if** D_p smaller than threshold κ is true

6:         Terminate the signal acquisition process.

7:     **else**

8:         $p = p + 1$

9:     **end if**

10: **end for**

After convergence, $\boldsymbol{x_p^{(l-1)}}$ will be sufficiently close to $\boldsymbol{x_p^{(l-1)}}$, so that $||\boldsymbol{x_p}||_2^{2(\boldsymbol{w_p^{(l)}})} = \sum_{j=1}^N w_{p(j)}^{(l)} x_{p(j)}^2 = \sum_{j=1}^N ((x_{p(j)}^{(l-1)})^2 + \epsilon)^{\frac{\nu}{2}-1} \cdot x_{p(j)}^2$ would be close to $||\boldsymbol{x_p}||_v^v$. In order to provide stability and ensure that a zero-valued component in $\boldsymbol{x_p^{(l)}}$ does not strictly prohibit a nonzero estimate at the next iteration, $\epsilon > 0$ [38] is adopted to regularize the optimization problem in (7). To simplify the illustration of the proposed algorithm, we define a function F_ν as

$$F_\nu(\boldsymbol{x}, \boldsymbol{\Phi}, \boldsymbol{w}) := \left[\frac{1}{2} ||\boldsymbol{\Phi}\boldsymbol{x} - \boldsymbol{y}||_2^2 + \lambda \sum_{i=1}^N w_{(i)} x_{(i)}^2 \right], \quad (8)$$

Therefore, the estimate in each iteration is equal to

$$\boldsymbol{x_p^{(l)}} := \arg \min \ F_\nu(\boldsymbol{x_p}, \boldsymbol{\Phi_p}, \boldsymbol{w^{(l)}}), \quad (9)$$

which requires solving a least squares problem that can be expressed in this matrix form:

$$\boldsymbol{x_p^{(l)}} = \boldsymbol{W_p^{(l)}} \boldsymbol{\Phi_p}^t \left(\boldsymbol{\Phi_p} \boldsymbol{W_p^{(l)}} \boldsymbol{\Phi_p}^t + \lambda \boldsymbol{I} \right)^{-1} \boldsymbol{y_p}, \quad (10)$$

where $\boldsymbol{W_p^{(l)}}$ is the $N \times N$ diagonal matrix with $1/w_{p(i)}^{(l)}$ as the i-th diagonal element and $\boldsymbol{\Phi_p^t}$ refers to the transpose of the sensing matrix $\boldsymbol{\Phi_p}$. Once $\boldsymbol{x_p^{(l)}}$ is obtained, we then update the weights accordingly. Repeating the whole procedure of signal acquisition and reconstruction, a sequence of spectrum reconstruction by increasing the number of time intervals, i.e., $\boldsymbol{x_1}, \boldsymbol{x_2}, \ldots, \boldsymbol{x_p}$, would be obtained. We now analyze the stopping criterion of signal acquisition.

After each signal reconstruction process, the proposed algorithm decides whether the reconstruction of the original signal is accurate enough or not. If the reconstructed signal does not satisfy certain accuracy requirement of spectral detection, the algorithm should require more time intervals until the accuracy requirement is met. However, since the original signal $\boldsymbol{x}$ is unknown before the reconstruction in real-world, the exact reconstruction error $e = ||\boldsymbol{x} - \boldsymbol{x_p}||_2^2$, could not be obtained to determine how accuracy the reconstructed signal is. Therefore, we measure the reconstruction error e indirectly and set stopping criterion in such a practical way. As the compressive samples vector $\boldsymbol{y_p}$ could be treated as the linear projection of the original signal $\boldsymbol{x}$ during the sampling process in (2), the Euclidean distance D_p between the sampling result obtained by applying the same linear function, i.e., sensing matrix, to the reconstructed signal, and the actual compressive samples should not be too far, otherwise we shall tell the reconstructed signal $\boldsymbol{x_p}$ is quite different from the original signal $\boldsymbol{x}$ with high probability. Specifically, the proposed Euclidean distance D_p is defined as

$$D_p = ||\boldsymbol{\Phi_{\Delta M}} \boldsymbol{x_p} - \Delta \boldsymbol{y_{p+1}}||_2^2, \quad (11)$$

and $\Delta \boldsymbol{y_{p+1}}$ is obtained by

$$\Delta \boldsymbol{y_{p+1}} = \boldsymbol{\Phi_{\Delta M}} \boldsymbol{x} + \boldsymbol{\xi}, \quad (12)$$

where $\boldsymbol{\Phi_{\Delta M}}$ denotes a $\Delta M \times N$ matrix. The Johnson-Lindenstrauss Lemma presented in [39] asserts that a high-dimensional space can be projected into a low-dimensional signal, where the dimension is equal or larger than $O(\zeta^{-2} \log N)$ so that all distances are preserved up to a multiplicative factor between $1 - \zeta$ and $1 + \zeta$ with $0 < \zeta \leq 1/2$. Therefore, we demonstrate the rigorous relationship between the proposed Euclidean distance D_p and the actual reconstruction error e by proving the point that $e = ||\boldsymbol{x} - \boldsymbol{x_p}||_2^2$ calculated in high-dimensional, i.e., dimension of $\boldsymbol{x_p}$, could be projected into D_p calculated in low-dimensional, i.e., dimension of $\Delta \boldsymbol{y_{p+1}}$, within the boundary factor of $1 \pm \zeta$ in Theorem 1. If the proposed Euclidean distance D_p is larger than the given threshold, the algorithm would continue the signal acquisition, otherwise the acquisition is terminated. For a given threshold κ which is predefined according to the reconstruction accuracy requirement, the minimum sensing time of the wideband signals would adapt to the actual sparsity levels of the spectrum. The outline of the proposed algorithm is summarized in Algorithm 1.

B. Theoretical guarantee

In theorem 1, we prove that the actual reconstruction error e could be estimated by the proposed Euclidean distance D_p within the boundary factor of $1 \pm \zeta$.

Theorem 1. *Given multiplicative factor $\zeta \in (0, 1/2]$, $\gamma \in (0, 1)$ and $\Delta M \leq C \zeta^{-2} log(1/2\gamma)$, we have*

$$Prob \left[\frac{D_p}{(1+\zeta)} \leq e \leq \frac{D_p}{(1-\zeta)} \right] \geq 1 - \gamma, \quad (13)$$

where the parameter C depends on the concentration property of random variables in measurement matrix $\boldsymbol{\Phi_{\Delta M}}$ [39]. D_p and e are defined as before.

Proof. With the aid of Johnson-Lindenstrauss Lemma, if the number of row r in $\boldsymbol{\Phi_{\Delta M}}$ is equal or larger than $C\zeta^{-2}\log(1/2\gamma)$, we have

$$(1-\zeta)\|\boldsymbol{X}\|_2^2 \leq \|\boldsymbol{\Phi_{\Delta M}X}\|_2^2 \leq (1+\zeta)\|\boldsymbol{X}\|_2^2, \quad (14)$$

where $\zeta \in (0, 1/2]$ and $\gamma \in (0, 1)$. Then we replace $\boldsymbol{X}$ in (14) by $\boldsymbol{x} - \boldsymbol{x_p}$ and obtain

$$\begin{aligned}(1-\zeta)\|\boldsymbol{x}-\boldsymbol{x_p}\|_2^2 &\leq \|\boldsymbol{\Phi_{\Delta M}}(\boldsymbol{x}-\boldsymbol{x_p})\|_2^2 \\ &\leq (1+\zeta)\|\boldsymbol{x}-\boldsymbol{x_p}\|_2^2.\end{aligned} \quad (15)$$

Since measurement matrix $\boldsymbol{\Phi_{\Delta M}}$ could be seen as a linear projection from $\mathbb{R}^N$ to $\mathbb{R}^{\Delta M}$, we can transform (15) into

$$\begin{aligned}(1-\zeta)\|\boldsymbol{x}-\boldsymbol{x_p}\|_2^2 &\leq \|\boldsymbol{\Phi_{\Delta M}x_p} - \Delta\boldsymbol{y_{p+1}}\|_2^2 \\ &\leq (1+\zeta)\|\boldsymbol{x}-\boldsymbol{x_p}\|_2^2.\end{aligned} \quad (16)$$

Finally, to obtain the observation that $e = \|\boldsymbol{x}-\boldsymbol{x_p}\|_2^2$ could be bounded and estimated by $D_p = \|\boldsymbol{\Phi_{\Delta M}x_p} - \Delta\boldsymbol{y_{p+1}}\|_2^2$, we change the (16) to another form (17) and simplify it to (18):

$$\begin{aligned}\frac{1}{(1+\zeta)}\|\boldsymbol{\Phi_{\Delta M}x_p} - \Delta\boldsymbol{y_{p+1}}\|_2^2 &\leq \|\boldsymbol{x}-\boldsymbol{x}\|_2^2 \\ &\leq \frac{1}{(1-\zeta)}\|\boldsymbol{\Phi_{\Delta M}x_p} - \Delta\boldsymbol{y_{p+1}}\|_2^2,\end{aligned} \quad (17)$$

$$\frac{D_p}{(1+\zeta)} \leq e \leq \frac{D_p}{(1-\zeta)}. \quad (18)$$

Therefore, when the row number ΔM in $\boldsymbol{\Phi_{\Delta M}}$ is equal or larger than $C\zeta^{-2}\log(1/2\gamma)$, the distance between D_p and e could be bounded up to a multiplicative factor between $1 - \zeta$ and $1 + \zeta$. Hence, we could state that the actual reconstruction error e could be estimated by the proposed Euclidean distance D_p when ΔM is larger than a lower bound and D_p could be utilized as the stopping criterion of the algorithm. See Appendix for The proof of that (17) is satisfied with probability larger than $1 - \gamma$. ∎

V. CS-BASED THE PROPOSED BLIND COOPERATING USER SELECTION ALGORITHM

In this section, we present a CS-based blind cooperating user selection algorithm applied in the CBSD sensing network for selecting the SUs with high SNR in the proposed scheme without the degradation of the detection performance by utilizing fewer SUs.

A. Algorithm description

In a CBRS sensing network, not every SU could produce informative spectrum sensing results due to the different deployment scenarios of the SUs. Moreover, as the number of cooperating SUs grows, the energy efficiency of the network decreases [40] and the sensing performance of the network only marginally increases once the number of cooperating SUs is sufficiently large [41]. Therefore, it is not an optimal choice to cooperate all SUs no matter whether they have high detection capability or not. The optimal performance could be achieved by selectively cooperating among SUs with high sensing performance of the transmission signals [42] where the sensing performances of SUs are fundamentally limited
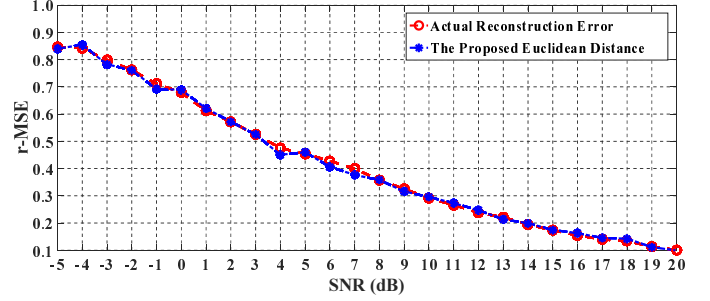

Fig. 3. r-MSE vs. average SNR between the actual reconstruction error and the estimated reconstruction error.

by the signal transmission channels since the reconstruction accuracy would be effected by the SNR of received signals.

As shown in Fig. 3, if the sampling rate is fixed and sufficient for signal reconstruction, reconstruction performance would be affected by the SNR of the transmission signal, which is likely caused by the channel fading, i.e., shadowing and multi-path. Therefore, CS could be utilized for cooperating user selection and the proposed autonomous CS-based spectrum sensing scheme could perform user selection without extra SNR estimation algorithms. The SUs with high SNR, could be selected by utilizing the proposed D_p to approximate the unknown reconstruction error. Specifically, the compressed samples vector $\boldsymbol{y}$ is divided into two vectors $\boldsymbol{y_r}$ ($\boldsymbol{y_r} \in \mathbb{R}^{r \times 1}$) and $\boldsymbol{y_v}$ ($\boldsymbol{y_v} \in \mathbb{R}^{v \times 1}$) for estimating the reconstruction error. According to the acquisition model in (2), these two vectors can be expressed as $\boldsymbol{y_r} = \boldsymbol{\Phi_r x} + \boldsymbol{\xi}$ and $\boldsymbol{y_v} = \boldsymbol{\Phi_v x} + \boldsymbol{\xi}$, respectively, where $\boldsymbol{x} \in \mathbb{R}^{N \times 1}$, $\boldsymbol{\Phi_r} \in \mathbb{R}^{r \times N}$ and $\boldsymbol{\Phi_v} \in \mathbb{R}^{v \times N}$. Parameter r as the number of compressed measurements in $\boldsymbol{y_r}$, is determined to ensure the successful reconstruction, and v is set to guarantee the sufficient accuracy of reconstruction error estimation as illustrated in Theorem 1. To select the suitable cooperating SUs, one can compare the estimated reconstruction error e^* with a predefined threshold which could be determined according to the detection capability requirement of SUs. Moreover, without the effort of signal reconstruction, only the locally collected samples should be sent to the fusion center for SUs selection under the centralized manner or be passed to other SUs under the distributed manner of the distributed CSS network.

VI. EXPERIMENTAL RESULTS

As a proof of concept for the proposed scheme, we verify the effectiveness of the proposed algorithms using both simulated signals and real-world signals in this section.

A. Experiment Setups and Performance Measures

Consider the simulated wideband signal $x(t) \in \mathcal{F} = [0, 500]$ MHz, whose DFT is denoted as $\boldsymbol{x_0^{\text{sim}}}$ which contains up to k active channels:

$$x(t) = \sum_{i=1}^k \sqrt{E_i B_i}\,\text{sinc}(B_i(t - t_i))e^{j2\pi f_i t} + n(t), \quad (19)$$
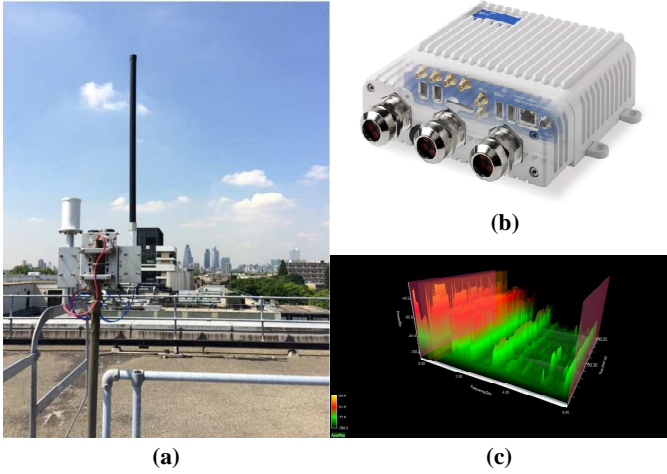
Fig. 4. (a) The outdoor antenna. (b) The RFeye node. (c) The captured power spectrum density at Queen Mary University of London [43].

where $\text{sinc}(x) = \sin(\pi x)/(\pi x)$, E_i, t_i and f_i represent the energy, the time offset, and the central frequency of the i-th sub-band and $n(t)$ denotes the noise. The i-th sub-band covers the frequency range $[f_i - \frac{B_i}{2}, f_i + \frac{B_i}{2}]$. Typically, the critical influences of a signal transmission channel consist of path loss, small-scale fading, e.g., multi-path, and large-scale fading, e.g., shadowing [26]. In each CBSD sensing network, the path loss could be approximately the same for all SUs since the maximum distance among SUs are assumed to be much smaller than the distance between the PUs and the SUs. For the fading effects, the multi-path effect exhibits a Rayleigh distribution, which could cause random variations in the SNR at the SUs, while the shadowing effect could be viewed as extra losses via a series of obstacles which is notoriously hard to model accurately and its statistics can vary widely with the deployment environments [41]. Therefore, we assume the SNR is varying in some channels for the different SUs in order to model both the large-scale and the small-scale fading effects.

To demonstrate the effectiveness of the proposed scheme over the wideband spectrum with the varying bandwidths and power levels of primary signals, the bandwidths B_i of i-th primary signal is varying from 5 to 20 MHz and the corresponding central frequency f_i is randomly located in $[\frac{B_i}{2}, W - \frac{B_i}{2}]$. The total sensing time is assumed as $T = 10 \mu s$, and thus the number of samples collected by the Nyquist sampling rate could be calculated as $N = T \cdot f_{NYQ}$. Rather than using the Nyquist sampling rate $f_{NYQ} \geq 2W = 1000$ MHz, we adopt the sub-Nyquist sampling rate $f_s < 2W$ which is depended on the maximum sparsity level $s_{\max}$ that can be estimated by long-term spectral observations. In the conventional CS approaches, the number of compressive samples $M = T \cdot f_s = K_0 s_{\max} \log(N/s_{\max})$ [15] should be determined by the worst case of sparsity level $s_{\max}$ to guarantee a very high acceptable reconstruction frequencies over the total sensing time T since the actual sparsity level is unknown in the real-world. In the proposed scheme, the total sensing time T is divided into $P = T \cdot f_s / \Delta M$ time intervals, where $P \in \mathbb{Z}^+$. The signal acquisition process would be terminated once the stopping criterion is reached. Therefore, the actual sensing

time of the proposed scheme is equal or lower than T. The rest of sensing time could be utilized for data transmission besides, the shorter sensing time would prevent the further interference to the PUs.

The real-world signals $\boldsymbol{x}_0^{\text{real}}$ are received by an RFeye node, which is an intelligent spectrum monitoring system that can provide real-time 24/7 monitoring of the radio spectrum [44]. As shown in Fig. 4, the RFeye node is located at Queen Mary University of London (51.523021°N 0.041592°W), and the antenna height is about 15 meters above ground.

To measure the reconstruction accuracy, we present the reconstruction error $||\boldsymbol{x}^* - \boldsymbol{x}_0||_2^2$ by the conventional average relative mean square error (r-MSE):

$$\text{r-MSE} = \frac{||\boldsymbol{x}^* - \boldsymbol{x}_0||_2^2}{||\boldsymbol{x}_0||_2^2}, \qquad (20)$$

where $\boldsymbol{x}^*$ denotes the reconstructed signal, $\boldsymbol{x}_0 = \boldsymbol{x}_0^{\text{sim}}$ in the simulation mode and $\boldsymbol{x}_0 = \boldsymbol{x}_0^{\text{real}}$ in the real-time mode. To quantify the detection performance we compute the detection probability, i.e., the fraction of occupied channels correctly being reported as occupied. The estimated active channel set is compared against the original signal support to compute the detection probability under 2000 trials.

B. Results over Simulated Signals

To prove the effectiveness of the proposed scheme and verify the theoretical results in Theorem 1, we compare the actual reconstruction error and the proposed Euclidean distance D_p which is referred as stopping criterion with the different number of time intervals in Fig. 5. It shows that the original signal is successfully reconstructed and the signal acquisition could be terminated at the time interval $p = 10$, rather than $p = 50$ (total sensing time) by the conventional CS-based algorithms. Since the proposed Euclidean distance D_p become very close to the actual reconstruction error when the actual reconstruction error becomes sufficiently small, D_p could be utilized as the stopping criterion to terminate the signal acquisition process as presented in Theorem 1. Moreover, Fig. 5 shows that the reconstruction accuracy could not be significantly improved by collecting additional samples. Therefore, the proposed scheme utilizes less sensing time than that of conventional CS approaches with the same sub-Nyquist sampling rate. The remaining sensing time can be utilized for future data transmission, besides, the shorter sensing time would prevent the further interference to the PUs.

Since the PUs and the SUs could randomly enter or leave the shared spectrum, the sparsity levels of the received wideband signals in practice are unknown and fluctuant. A practical CS-based sensing algorithm should be robust against different signal sparsity levels. Therefore, in Fig. 6, we demonstrate the performance of the proposed scheme under the different sparsity levels with a fix sampling rate $f_s = 0.5 f_{NYQ}$. From Fig. 6, it can be observe that the proposed scheme could successfully reconstruct the signals and terminate the sensing process at the time interval $p = 8, 15, 20$ under the sparsity levels $s = 0.05N, 0.10N, 0.15N$, where the higher sparsity levels of the signals would lead to the more time
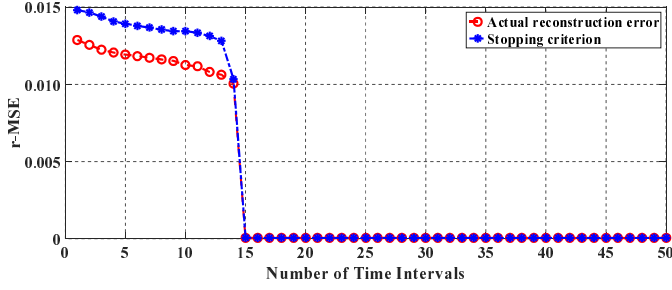
Fig. 5. r-MSE vs. number of time intervals between the actual reconstruction error and the stopping criterion D_p when sparsity level is fixed as $s = 0.1N$ for the proposed scheme.
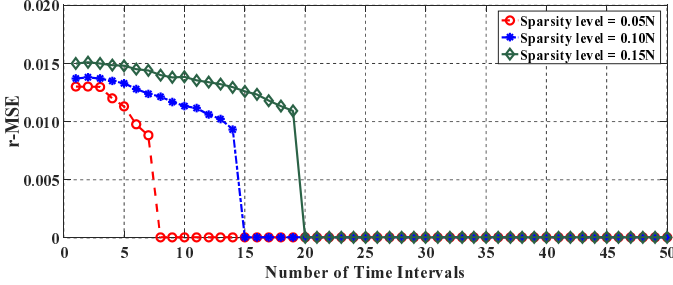

Fig. 6. r-MSE vs. number of time intervals under different sparsity levels $s = 0.05N, 0.10N, 0.15N$ for the proposed scheme.
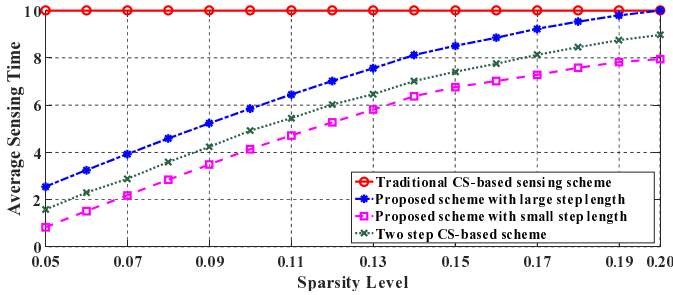

Fig. 7. Average sensing time (μs) vs. the sparsity level (N) between the proposed scheme and other CS-based spectrum sensing algorithms.

intervals needed for guaranteeing the reconstruction accuracy. Therefore, without the prior knowledge of the actual spectral sparsity, the proposed scheme can autonomously adopt a proper number of time intervals for signal reconstruction.

In Fig. 7, we present the comparison among the two-step CS-based spectrum sensing scheme [24] (termed two-step CS-based scheme), the conventional compressive spectrum sensing scheme [45] (termed traditional CS-based scheme) and the proposed scheme. We use the average sensing time in μs instead of the number of time intervals to measure the reduction of the sensing cost, since only the proposed scheme needs to divide the total sensing time into multiple small time intervals. Without loss of generality, we test different schemes with a fixed sampling rate $f_s = 0.5f_{NYQ}$. To illustrate the impact of adopting different step lengths ΔM, the proposed scheme is tested with both the large step length and with the small step length, which adopts $\Delta M = 500$ and $\Delta M = 50$, respectively. It is shown in Fig. 7 that the performance of the proposed scheme is influenced by the step length ΔM.
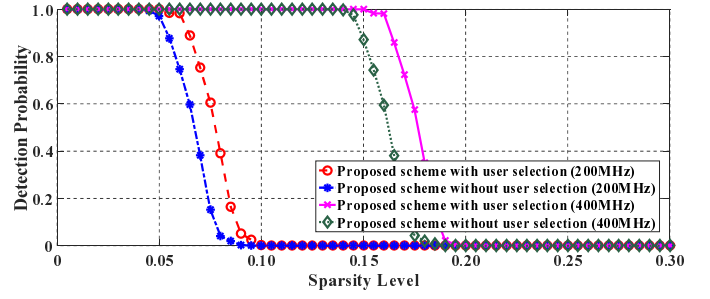

Fig. 8. Detection probability vs. the sparsity level (N) between the proposed algorithm with and without cooperating user selection under different sampling rates = 200MHz and 400MHz.

If the ΔM is too large, the proposed scheme will lose its advantage and be worse than the two-step CS-based scheme. To understand this, we consider an extreme setting: the total number of time intervals is set to 1 and thus the step length become $\Delta M = M = T \cdot f_s$, where the proposed scheme is degraded to the conventional compressive spectrum sensing scheme which could not work with unknown sparsity levels efficiently. Therefore, ΔM should not be too large in order to keep the effectiveness of the proposed scheme. However, if ΔM is too small, it will require many steps, e.g., maximum 250 time intervals are required if $\Delta M = 20$ in this simulation, although it is more likely to reach the minimum sensing time. Therefore, there is a trade-off need to be balanced between computational complexity and the effectiveness of the proposed scheme.

To illustrate the functionality of the proposed CS-based blind cooperating user selection algorithm, we show the detection probability against the sparsity level between the proposed scheme with and without cooperating user selection under different sampling rates (200 MHz and 400MHz) in Fig. 8. In the proposed scheme, we select half of the SUs to perform CSS for demonstration purpose. The maximum number of the cooperating SUs could be set according to the capacity in the practical network environment. It is shown that the detection probability of the proposed scheme with user selection is always higher than or equal to that of the proposed scheme without user selection. Therefore, there is no degeneration of the detection probability when cooperating with fewer SUs. Moreover, the detection probability is improved when sparsity level of the wideband spectrum is high, i.e., higher occupancy ratio, under different sampling rates. That is because the proposed cooperating user selection scheme could take out the SUs with bad detection results, e.g., malicious users, which could affect the overall detection performance.

C. Analysis on Real-world Signals

To analyze the performance of the proposed scheme with real-world signals over the different spectrums, e.g., TVWS spectrum and 3.5GHz spectrum in the UK, we compare the r-MSE of the proposed scheme against the two-step CS-based spectrum sensing scheme with the same sampling rate in Fig. 9. It is shown that the proposed scheme not only can work properly in the 3.5GHz shared spectrum, but also can

deal with the TVWS spectrum. Particularly, as the real-world 3.5GHz spectrum is much sparser than the TVWS spectrum in the UK, the required sensing time of the 3.5GHz spectrum is less than that of the TVWS spectrum. The proposed method outperforms the two-step CS in terms of sensing time under give sampling rate since the adopted AR-IRLS reconstruction algorithm requires fewer compressive samples to achieve the same reconstruction accuracy compared with the basis pursuit denoising (BPDN) reconstruction algorithm adopted in two-step CS [37]. The proposed scheme is suitable for the practical measurements and can be extended to other shared spectrums like TVWS and the bands with the higher central frequencies.

VII. CONCLUSION

In this paper, we have proposed an autonomous CS augmented spectrum sharing scheme to provide more efficient spectrum opportunities identification within the CBSD sensing network. In order to tackle the challenges of realizing the CBSD sensing network, firstly we proposed an autonomous CS-based sensing algorithm which enables the local SUs to automatically choose the minimum sensing time while guaranteeing the exact wideband signal reconstruction. To enhance the detection performance and use fewer SUs in each CBSD sensing network, a CS-based blind cooperating user selection algorithm is proposed to select the SUs which could produce informative spectrum sensing results according to the detection SNR of the transmission signals. The robust performance of the proposed CS-based autonomous sensing scheme has also been validated over both simulated signals and real-world signals recorded by the RFeye node at QMUL. Numerical analysis and experimental results have shown that the proposed scheme could not only adaptively select an appropriate number of time intervals without the estimation of sparsity level but also offer exact signal reconstruction for varying bandwidth of channels and power levels under different unknown sparsity levels. In comparison with conventional compressive spectrum sensing schemes and two-step CS-based spectrum sensing schemes, it is shown that the proposed scheme can achieve the better detection performance as well as the shorter sensing time and fewer number of cooperating SUs. Additionally, the remaining sensing time can be utilized for data transmission and avoiding the further interference to the ongoing primary transmissions. These benefits enable the proposed scheme to be implementable for spectrum sharing, especially over the 3.5GHz spectrum and the higher frequencies. Moreover, we shall extend the proposed scheme with advanced detector such as frequency domain autocorrelation [22] and maximum - minimum energy detection sensing algorithm [46] to further enhance the ability against the noise uncertainty and frequency selective channel in future work.

APPENDIX
PROOF OF THE THEOREM 1

Let $\boldsymbol{X} \in \mathbb{R}^n$ be an arbitrary fixed unit vector, i.e., $||\boldsymbol{X}||_2^2 = 1$ for simplicity, and the linear projection $\boldsymbol{X} \rightarrow \boldsymbol{Y}$ is defined by

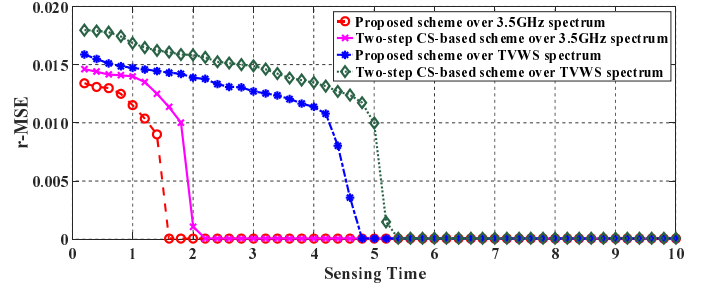$$Y_{(i)} = \sum_{j=1}^{n} A_{(ij)} X_{(j)}, \qquad i = 1, 2, \ldots, r, \qquad (21)$$

Fig. 9. r-MSE vs. the sensing time (μs) over different real-world spectrum signals.

where $A_{(ij)}$ are independent random variables with $\mathrm{E}[A_{(ij)}] = 0$ and $\mathrm{Var}[A_{(ij)}] = 1$, which has an uniform sub-Gaussian tail. Since $\boldsymbol{Y}$ could be seen as a linear combination of the $\boldsymbol{A_{(i)}}$ which is the i-th row of $\boldsymbol{A}$, $Y_{(i)}$ has an uniform sub-Gaussian tail as well. Therefore, according to the Proposition 3.2 in [39], we could define a random variable as

$$Z = \frac{1}{\sqrt{r}}(Y_{(1)}^2 + \cdots + Y_{(r)}^2 - r), \qquad (22)$$

where Z has a sub-Gaussian tail up to $\sqrt{r}$. Therefore, $||\boldsymbol{Y}||_2^2 - 1$ is distributed as $Z/\sqrt{r}$ and we can get

$$\begin{aligned} \mathrm{Prob}[||\boldsymbol{Y}||_2 \geq 1 + \zeta] &= \mathrm{Prob}[||\boldsymbol{Y}||_2^2 \geq 1 + \zeta^2 + 2\zeta] \\ &\leq \mathrm{Prob}[||\boldsymbol{Y}||_2^2 \geq 1 + 2\zeta] \qquad (23) \\ &= \mathrm{Prob}[Z \geq 2\zeta\sqrt{r}]. \end{aligned}$$

As $\zeta \in (0, 1/2]$, by utilizing the Chernoff-type inequality, we have

$$\mathrm{Prob}[Z \geq 2\zeta\sqrt{r}] \leq \exp^{-a(2\zeta\sqrt{r})^2} = \exp^{-4a\zeta^2 C\zeta^{-2}\log(2/\gamma)} \leq \frac{\gamma}{2} \qquad (24)$$

for $C \geq 1/2a$. Applying the same principle and the similar calculation as above, $\mathrm{Prob}[||\boldsymbol{Y}||_2 \leq 1 - \zeta] \leq \gamma/2$ could be demonstrated as well. Therefore, we can get the conclusion that

$$\mathrm{Prob}\left[(1-\zeta)||\boldsymbol{X}||_2^2 \leq ||\boldsymbol{AX}||_2^2 \leq (1+\zeta)||\boldsymbol{X}||_2^2\right] \geq 1 - \gamma. \qquad (25)$$

Then we replace $\boldsymbol{X}$ in (25) by $\boldsymbol{x} - \boldsymbol{x_p}$ to obtain (26). As $\boldsymbol{A}$ refer to the linear projection $\boldsymbol{X} \rightarrow \boldsymbol{Y}$, we could get (27) and its another form (28), shown below:

$$\begin{aligned} \mathrm{Prob}\big[(1-\zeta)||\boldsymbol{x} - \boldsymbol{x_p}||_2^2 &\leq ||\boldsymbol{\Phi_{\Delta M}}(\boldsymbol{x} - \boldsymbol{x_p})||_2^2 \\ &\leq (1+\zeta)||\boldsymbol{x} - \boldsymbol{x_p}||_2^2\big] \geq 1 - \gamma, \end{aligned} \qquad (26)$$

$$\begin{aligned} \mathrm{Prob}\big[(1-\zeta)||\boldsymbol{x} - \boldsymbol{x_p}||_2^2 &\leq ||\boldsymbol{\Phi_{\Delta M}}\boldsymbol{x_p} - \Delta\boldsymbol{y_{p+1}}||_2^2 \\ &\leq (1+\zeta)||\boldsymbol{x} - \boldsymbol{x_p}||_2^2\big] \geq 1 - \gamma, \end{aligned} \qquad (27)$$

$$\mathrm{Prob}\left[\frac{1}{(1+\zeta)}||\boldsymbol{\Phi_{\Delta M}}\boldsymbol{x_p} - \Delta\boldsymbol{y_{p+1}}||_2^2 \leq ||\boldsymbol{x} - \boldsymbol{x^*}||_2^2 \right.$$
$$\left. \leq \frac{1}{(1-\zeta)}||\boldsymbol{\Phi_{\Delta M}}\boldsymbol{x_p} - \Delta\boldsymbol{y_{p+1}}||_2^2\right] \geq 1 - \gamma. \qquad (28)$$

Finally, we shall simplify (28) to the result

$$\mathrm{Prob}\left[\frac{D_p}{(1+\zeta)} \leq e \leq \frac{D_p}{(1-\zeta)}\right] \geq 1 - \gamma. \qquad (29)$$

REFERENCES

[1] G. Ding, J. Wang, Q. Wu, Y.-D. Yao, F. Song, and T. A. Tsiftsis, "Cellular-Base-Station-Assisted Device-to-Device Communications in TV White Space," *IEEE J. Sel. Areas Commun.*, vol. 34, no. 1, pp. 107–121, Jan. 2016.

[2] F. Yang, J. Li, T. Lei, and S. Wang, "Architecture and key technologies for internet of vehicles: a survey," *Journal of Commun. and Inf. Netw.*, vol. 2, no. 2, pp. 1–17, Jun. 2017.

[3] J. Holdren and E. Lander, "Report to the President: Realizing the Full Potential of Government-Held Spectrum to Spur Economic Growth," Presidents Council Advisors Sci. Technol., Washington, DC, USA, Tech. Rep., 2012.

[4] Agre, Jonathan R. and Gordon, Karen D. (Sept. 2015). *Summary of Recent Federal Government Activities to Promote Spectrum Sharing*. [Online]. Available: https://www.ida.org/idamedia/Corporate/Files/Publications/STPIPubs/2015/p5186final.pdf

[5] W. Zhang, R. K. Mallik, and K. B. Letaief, "Optimization of cooperative spectrum sensing with energy detection in cognitive radio networks," *IEEE Trans. Wireless Commun.*, vol. 8, no. 12, pp. 5761–5766, Dec. 2009.

[6] Z. Quan, S. Cui, A. H. Sayed, and H. V. Poor, "Optimal multiband joint detection for spectrum sensing in cognitive radio networks," *IEEE Trans. Signal Process.*, vol. 57, no. 3, pp. 1128–1140, Mar. 2009.

[7] Y. Gao, Z. Qin, Z. Feng, Q. Zhang, O. Holland, and M. Dohler, "Scalable & reliable IoT enabled by dynamic spectrum management for M2M in LTE-A," *IEEE Internet of Things Journal*, vol. 3, no. 6, pp. 1135 – 1145, May 2016.

[8] Office of Commun., "3.8 GHz to 4.2 GHz band: Opportunities for Innovation," Office of Commun., London, UK, Final Rep., Apr. 2016.

[9] Fed. Commun. Commission, "Amendment of the Commission's Rules with Regard to Commercial Operations in the 3550-3650 MHz Band," Washington, DC, USA, Tech. Rep. GN Docket No. 12-354, Apr. 2014.

[10] Office of Commun., "A framework for spectrum sharing," Office of Commun., London, UK, Final Rep., Apr. 2016.

[11] O. Holland, S. Ping, Y. Gao, Z. Qin, A. Aijaz, J. Chareau, P. Chawdhry, and H. Kokkinen, "To white space or not to white space: That is the trial within the ofcom TV white spaces pilot," in *Proc. IEEE Int. Conf. on Dynamic Spectrum Access Netw. (DYSPAN)*, Stockholm, Sweden, Sep. 2015, pp. 11–22.

[12] Z. Qin, Y. Gao, and C. G. Parini, "Data-assisted low complexity compressive spectrum sensing on real-time signals under sub-Nyquist rate," *IEEE Trans. Wireless Commun.*, vol. 15, no. 2, pp. 1174–1185, Feb. 2016.

[13] Z. Qin, Y. Gao, M. Plumbley, and C. Parini, "Wideband spectrum sensing on real-time signals at sub-Nyquist sampling rates in single and cooperative multiple nodes," *IEEE Trans. Signal Process.*, vol. 64, no. 12, pp. 3106–3117, Jun. 2016.

[14] T. T. Nguyen, A. Sahoo, M. R. Souryal, and T. A. Hall, "3.5 GHz environmental sensing capability sensitivity requirements and deployment," in *Proc. IEEE Int. Symp. on Dynamic Spectrum Access Networks (DySPAN)*, Piscataway, NJ, May 2017, pp. 1–10.

[15] D. L. Donoho, "Compressed sensing," *IEEE Trans. Inf. Theory*, vol. 52, no. 4, pp. 1289–1306, Apr. 2006.

[16] Z. Tian and G. B. Giannakis, "Compressed sensing for wideband cognitive radios," in *Proc. IEEE Int. conf. on Acoust., Speech and Signal Process. (ICASSP)*, Honolulu, HI, Apr. 2007, pp. 1357–1360.

[17] X. Zhang, Y. Ma, and Y. Gao, "Autonomous compressive spectrum sensing approach for 3.5 GHz shared spectrum," in *Proc. IEEE Int. conf. on Signal and Inf. Process. (GlobalSIP)*, Washington, D.C., Dec. 2016.

[18] Q. Song and W. Hamouda, "Performance analysis and optimization of multiselective scheme for cooperative sensing in fading channels," *IEEE Trans. Veh. Technol.*, vol. 65, no. 1, pp. 358–366, Jan. 2016.

[19] L. Qian, J. Zhu, and S. Zhang, "Survey of wireless big data," *Journal of Commun. and Inf. Netw.*, vol. 2, no. 1, pp. 1–18, Mar. 2017.

[20] E. Peh and Y.-C. Liang, "Optimization for cooperative sensing in cognitive radio networks," in *Wireless Communications and Networking Conference, 2007. WCNC 2007. IEEE*, Hong Kong, Mar. 2007, pp. 27–32.

[21] S. Dikmese, Z. Ilyas, P. Sofotasios, M. Renfors, and M. Valkama, "Novel frequency domain cyclic prefix autocorrelation based compressive spectrum sensing for cognitive radio," in *Proc. IEEE Int. conf. on Vehicular Technology (VTC-Spring)*, Nanjing, China, May 2016, pp. 1–6.

[22] S. Dikmese, Z. Ilyas, P. C. Sofotasios, M. Renfors, and M. Valkama, "Sparse frequency domain spectrum sensing and sharing based on cyclic prefix autocorrelation," *IEEE J. Sel. Areas Commun.*, vol. 35, no. 1, pp. 159–172, Jan. 2017.

[23] Y. Ma, X. Zhang, and Y. Gao, "Joint Sub-Nyquist Spectrum Sensing Scheme with Geolocation Database over TV White Space," *IEEE Trans. Veh. Technol.*, Oct. 2017 (To appear).

[24] Y. Wang, Z. Tian, and C. Feng, "Sparsity order estimation and its application in compressive spectrum sensing for cognitive radios," *IEEE Trans. Wireless Commun.*, vol. 11, no. 6, pp. 2116–2125, Jun. 2012.

[25] X. Zhang, Z. Qin, and Y. Gao, "Dynamic adjustment of sparsity upper bound in wideband compressive spectrum sensing," in *Proc. IEEE Int. conf. on Signal and Inf. Process. (GlobalSIP)*, Atlanta, GA, Dec. 2014, pp. 1214–1218.

[26] Y. Selén, H. Tullberg, and J. Kronander, "Sensor selection for cooperative spectrum sensing," in *Proc. IEEE Int. Symp. on Dynamic Spectrum Access Networks (DySPAN)*, Chicago, Oct. 2008, pp. 1–11.

[27] Z. Khan, J. Lehtomaki, K. Umebayashi, and J. Vartiainen, "On the selection of the best detection performance sensors for cognitive radio networks," *IEEE Signal Process. Lett.*, vol. 17, no. 4, pp. 359–362, Apr. 2010.

[28] A. S. Cacciapuoti, I. F. Akyildiz, and L. Paura, "Correlation-aware user selection for cooperative spectrum sensing in cognitive radio ad hoc networks," *IEEE J. Sel. Areas Commun.*, vol. 30, no. 2, pp. 297–306, Feb. 2012.

[29] Q.-T. Vien, H. X. Nguyen, R. Trestian, P. Shah, and O. Gemikonakli, "A hybrid double-threshold based cooperative spectrum sensing over fading channels," *IEEE Trans. Wireless Commun.*, vol. 15, no. 3, pp. 1821–1834, Nov. 2016.

[30] Y. Ma, Y. Gao, Y.-C. Liang, and S. Cui, "Reliable and efficient sub-Nyquist wideband spectrum sensing in cooperative cognitive radio networks," *IEEE J. Sel. Areas Commun.*, vol. 34, no. 10, pp. 2750–2762, Oct. 2016.

[31] J. A. Tropp, J. N. Laska, M. F. Duarte, J. K. Romberg, and R. G. Baraniuk, "Beyond nyquist: Efficient sampling of sparse bandlimited signals," *IEEE Trans. Inf. Theory*, vol. 56, no. 1, pp. 520–544, Jan. 2010.

[32] M. Mishali and Y. C. Eldar, "From theory to practice: Sub-nyquist sampling of sparse wideband analog signals," *IEEE J. Sel. Signal Process.*, vol. 4, no. 2, pp. 375–391, Apr. 2010.

[33] J. A. Tropp and S. J. Wright, "Computational methods for sparse solution of linear inverse problems," *Proc. IEEE*, vol. 98, no. 6, pp. 948–958, Apr. 2010.

[34] J. Yang, J. Wright, T. S. Huang, and Y. Ma, "Image super-resolution via sparse representation," *IEEE Trans. Image Process.*, vol. 19, no. 11, pp. 2861–2873, Nov. 2010.

[35] M. Wang, W. Xu, and A. Tang, "On the performance of sparse recovery via l_p-minimization," *IEEE Trans. Inf. Theory*, vol. 57, no. 11, pp. 7255–7278, Nov. 2011.

[36] I. Daubechies, R. DeVore, and M. Fornasier, "Iteratively reweighted least squares minimization for sparse recovery," *Commun. Pure Appl. Math.*, vol. 63, no. 1, pp. 1–38, Jan. 2010.

[37] X. Zhang, Y. Ma, Y. Gao, and S. Cui, "Real-time adaptively-regularized compressive sensing in cognitive radio networks," *IEEE Trans. Veh. Technol.*, vol. PP, no. 99, pp. 1–1, 2017.

[38] R. Chartrand and V. Staneva, "Restricted isometry properties and non-convex compressive sensing," *Inverse Problems*, vol. 24, no. 035020, pp. 1–14, May 2008.

[39] J. Matoušek, "On variants of the johnson-lindenstrauss lemma," *Random Struct. & Algorithms*, vol. 33, no. 2, pp. 142–156, Sep. 2008.

[40] Y.-C. Liang, Y. Zeng, E. C. Y. Peh, and A. T. Hoang, "Sensing-throughput tradeoff for cognitive radio networks," *IEEE Trans. Wireless Commun.*, vol. 7, no. 4, pp. 1326–1337, Apr. 2008.

[41] S. M. Mishra, A. Sahai, and R. W. Brodersen, "Cooperative sensing among cognitive radios," in *Proc. IEEE Int. Conf. on Commun. (ICC)*, Malaysia, Jun. 2006, pp. 1658–1663.

[42] L. Lu, X. Zhou, U. Onunkwo, and G. Y. Li, "Ten years of research in spectrum sensing and sharing in cognitive radio," *EURASIP Journal on Wireless Commun. and Netw.*, vol. 2012, no. 1, p. 28, Jan. 2012.

[43] X. Zhang, Y. Ma, and Y. Gao, "Adaptively regularized compressive spectrum sensing from real-time signals to real-time processing," in *Proc. IEEE Global Commun. Conf. (GLOBECOM)*, Washington, D.C., Dec. 2016.

[44] CRFS. (Oct. 2015). *RFeye Node*. [Online]. Available: https://uk.crfs.com/zh-hans/products/rfeyenode/node-20-6/

[45] H. Sun, A. Nallanathan, C.-X. Wang, and Y. Chen, "Wideband spectrum sensing for cognitive radio network: a survey," *IEEE Trans. Wireless Commun.*, vol. 20, no. 2, pp. 74–81, Apr. 2013.

[46] S. Dikmese, P. C. Sofotasios, M. Renfors, and M. Valkama, "Maximum-minimum energy based spectrum sensing under frequency selectivity for cognitive radios," in *Cognitive Radio Oriented Wireless Networks and Communications (CROWNCOM), 2014 9th International Conference on*, Oulu, Finland, Jun. 2014, pp. 347–352.
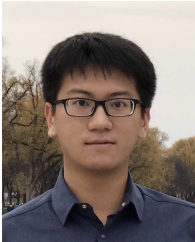
Xingjian Zhang (S'16) received the B.Sc. degree (First Class Hons.) in telecommunications engineering from Beijing University of Posts and Telecommunications, Beijing, China. He is currently working towards his Ph.D. degree in the School of Electronic Engineering and Computer Science, Queen Mary University of London since 2014. His current research interests include cooperative wireless sensor networks, compressive sensing, real-time spectrum monitoring and analysis, and Internet of things (IoT) applications.

Yuan Ma (S'15-M'17) received the B.Sc. degree (First Class Hons.) in telecommunications engineering from Beijing University of Posts and Telecommunications, Beijing, China, and the Ph.D. degree in electronic engineering from Queen Mary University of London, London, U.K., in 2013 and 2017, respectively. She is currently an Assistant Professor with the College of Information Engineering, Shenzhen University, Shenzhen, China. Her research interests include cognitive and cooperative wireless networking, sub-Nyquist signal processing, and spectrum analysis, detection, and sharing over TV white space.

Yue Gao (S'03-M'07-SM'13) is a Reader in Antennas and Signal Processing, and Director of Whitespace Machine Communication Lab in the School of Electronic Engineering and Computer Science at Queen Mary University of London (QMUL) in the UK. He worked as Research Assistant, Lecturer and Senior Lecturer at QMUL after having received his PhD degree from QMUL in 2007. He is currently leading a team developing theoretical research into practice in the interdisciplinary area among smart antennas, signal processing, spectrum sharing and internet of things (IoT) applications. He has published over 140 peer-reviewed journal and conference papers, 2 patents, and 2 book chapters. He is a co-recipient of the EU Horizon Prize Award on Collaborative Spectrum Sharing in 2016, and Research Performance Award from Faulty of Science and Engineering at QMUL in 2017. He is an Engineering and Physical Sciences Research Council (EPSRC) Fellow from 2018 - 2023.

He is an Editor for the IEEE Transactions on Vehicular Technology, IEEE Wireless Communication Letter and China Communications. He is serving as Cognitive Radio Symposium Co-Chair of the IEEE GLOBECOM 2017. He served as the Signal Processing for Communications Symposium Co-Chair for IEEE ICCC 2016, Publicity Co-Chair for IEEE GLOBECOM 2016, and General Chair of the IEEE WoWMoM and iWEM 2017. He is a Senior Member of IEEE, a Secretary of the IEEE Technical Committee on Cognitive Networks, and an IEEE Distinguished Lecturer of Vehicular Technology Society.

Wei Zhang (S'01-M'06-SM'11-F'15) received the Ph.D. degree in electronic engineering from the Chinese University of Hong Kong, Hong Kong, in 2005. He was a Research Fellow with the Hong Kong University of Science and Technology, Clear Water Bay, Hong Kong, from 2006 to 2007. He is currently a Professor with the University of New South Wales, Sydney, NSW, Australia. His research interests include cognitive radio, 5G, heterogeneous networks, and massive multiple input and multiple output. He is the Editor-in-Chief of the IEEE WIRELESS COMMUNICATIONS LETTERS. He is also an Editor for the IEEE TRANSACTIONS ON COMMUNICATIONS. He served as an Editor for the IEEE TRANSACTIONS ON WIRELESS COMMUNICATIONS from 2010 to 2015 and the IEEE JOURNAL ON SELECTED AREAS IN COMMUNICATIONS (Cognitive Radio Series) from 2012 to 2014.

He participates actively in committees and conference organization for the IEEE Communications Society. He is Vice Chair for the IEEE Wireless Communications Technical Committee. He is an elected member of the SPCOM Technical Committee of the IEEE Signal Processing Society. He also served in the organizing committee of the 2016 IEEE International Conference on Acoustics, Speech and Signal Processing, Shanghai, China, and the IEEE GLOBECOM 2017, Singapore. He is TPC co-Chair of the 2017 Asia-Pacific Conference on Communications and the 2019 International Conference on Communications in China. He is a member of the Board of Governors of the IEEE Communications Society. He was a recipient of the IEEE Communications Society Asia-Pacific Outstanding Young Researcher Award 2009 and the IEEE ComSoc TCCN Publication Award 2017 as well as four best paper awards in international Conferences.